



Published in final edited form as:

Nat Cell Biol. ; 14(2): 192–200. doi:10.1038/ncb2408.

## Toll-like receptor activation suppresses endoplasmic reticulum stress-induced CHOP and translation inhibition through activation of eIF2B

Connie W. Woo<sup>1</sup>, Lydia Kutzler<sup>2</sup>, Scot R. Kimball<sup>2</sup>, and Ira Tabas<sup>1,3</sup>

<sup>1</sup>Departments of Medicine, Pathology & Cell Biology, and Physiology & Cellular Biophysics, Columbia University, New York, NY 10032

<sup>2</sup>Department of Cellular and Molecular Physiology, The Pennsylvania State University College of Medicine, Hershey, Pennsylvania 17033

### Abstract

Activation of toll-like receptors (TLRs) induces the endoplasmic reticulum (ER) Unfolded Protein Response (UPR) to accommodate essential protein translation<sup>1,2</sup>. However, despite increased p-eIF2 $\alpha$ , a TLR-TRIF-dependent pathway assures that the cells avoid CHOP induction, apoptosis, and translational suppression of critical proteins<sup>3</sup>. Because p-eIF2 $\alpha$  decreases the functional interaction of eIF2 with eIF2B, a guanine nucleotide exchange factor (GEF), we explored the hypothesis that TLR-TRIF signaling activates eIF2B-GEF activity to counteract the effects of p-eIF2 $\alpha$ . We now show that TLR-TRIF signaling activates eIF2B-GEF through PP2A-mediated Ser-dephosphorylation of the eIF2B  $\epsilon$ -subunit. PP2A itself is activated by decreased Src-family-kinase-induced Tyr-phosphorylation of its catalytic subunit. Each of these processes are required for TLR-TRIF-mediated CHOP suppression in ER-stressed cells *in vitro* and *in vivo*. Thus, in the setting of prolonged, physiologic ER stress, a unique TLR-TRIF-dependent translational control pathway enables cells to carry out essential protein synthesis and avoid CHOP-induced apoptosis while still benefitting from the protective arms of the UPR.

---

In cells undergoing ER stress, PERK phosphorylates eukaryotic initiation factor (eIF) 2 $\alpha$  (p-eIF2 $\alpha$ ), which decreases recycling of the essential ternary complex of eIF2, GTP, and tRNA<sub>i</sub><sup>Met</sup> and thereby decreases the translation initiation of most cellular mRNAs<sup>2</sup>. This action also enhances the translation of the mRNA encoding ATF4, which then induces CEBP-homologous protein (CHOP; GADD153)<sup>2</sup>. During physiologic ER stress, transient CHOP expression is beneficial, but in pathologically chronic ER stress, prolonged CHOP expression promotes cell death and has been implicated in a number of diseases, including

---

Users may view, print, copy, download and text and data- mine the content in such documents, for the purposes of academic research, subject always to the full Conditions of use: [http://www.nature.com/authors/editorial\\_policies/license.html#terms](http://www.nature.com/authors/editorial_policies/license.html#terms)

<sup>3</sup>Correspondence should be addressed to I.T. (iat1@columbia.edu).

#### AUTHOR CONTRIBUTIONS

C.W.W. performed the experiments and assisted with planning the experiments, data analysis, and writing the manuscript; L.K. assisted with planning the experiments and data analysis; S.R.K. assisted with planning the experiments, data analysis and writing the manuscript; I.T. coordinated the project and assisted with planning the experiments, data analysis, and writing the manuscript.

#### COMPETING FINANCIAL INTERESTS

The authors declare no competing financial interests.

neurodegenerative diseases, atherosclerosis, diabetes, and renal disease<sup>5,6</sup>. It therefore follows that in cells that require a *physiologic* uninterrupted UPR response, prolonged expression of CHOP and suppression of global protein synthesis would have to be at least partially abrogated. In the case of macrophages exposed to activators of TLR4 or TLR3, this function is effected by a pathway downstream of the adaptor TRIF that suppresses ATF4 translation and subsequent CHOP induction and maintains global translation in the face of *normal* PERK activation and eIF2 $\alpha$  phosphorylation<sup>3</sup>. When this pathway is blocked in mice, ER stress-induced CHOP induction, cell death, and organ dysfunction ensue<sup>3</sup>.

The goal of the current study was to elucidate the molecular signaling components of this adaptive pathway. The above findings suggested that the pathway somehow renders the cells “resistant” to p-eIF2 $\alpha$ , which functions by tightly binding an essential ternary complex GTP-exchange factor (GEF) called eIF2B in a manner that competitively inhibits GDP-GTP exchange on the  $\gamma$ -subunit of eIF2<sup>7</sup>. In this context, we explored the hypothesis that TLR-TRIF increases eIF2B GEF activity, which might enable adequate GDP-GTP exchange, in the face of p-eIF2 $\alpha$ .

We first determined whether TLR-TRIF signaling increases eIF2B GEF activity in ER-stressed cells. Macrophages from wild-type and *Trif*<sup>-/-</sup> mice were treated with the ER stressor tunicamycin alone or after pre-treatment of the cells with the TLR4 activator lipopolysaccharide (LPS). As expected from the increase in p-eIF2 $\alpha$  in ER-stressed cells<sup>4</sup>, tunicamycin suppressed eIF2B GEF activity in both wild-type and *Trif*<sup>-/-</sup> macrophages (**Figure 1a**). However, in LPS-treated wild-type but not *Trif*<sup>-/-</sup> ER-stressed macrophages, eIF2B GEF activity was increased to the control level. Thus, TLR-TRIF signaling restores ER stress-suppressed eIF2B GEF activity to the non-ER stress level.

One mechanism of eIF2B GEF activation is through dephosphorylation of a p-Ser residue (termed Ser<sup>GSK</sup> after the kinase that can phosphorylate it<sup>8</sup>) in the  $\epsilon$  subunit of the eIF2B<sup>8,9</sup>. LPS pre-treatment partially decreased the pSer<sup>GSK</sup>-eIF2B $\epsilon$  in both tunicamycin-treated cells and in untreated WT but not *Trif*<sup>-/-</sup> cells (**Figure 1b-c**). Thus, TRIF is required for the ability of LPS to both increase eIF2B GEF activity and to decrease eIF2B phosphorylation.

The hypothesis predicts that the need for LPS to suppress CHOP could be bypassed by increasing eIF2B GEF activity by an LPS-independent means. We tested this idea by transfecting MEFs with wild-type or S-A<sup>GSK</sup>-mutant rat *Eif2be*<sup>10</sup>, which should be particularly potent because it cannot be deactivated by phosphorylation (S. Kimball, unpublished data). We first showed that LPS suppresses p-eIF2B $\epsilon$ , CHOP, and CHOP promoter-driven GFP reporter expression in ER-stressed MEFs (**Figure S1a-b**), and CHOP suppression was not affected by the transfection reagent, Lipofectamine (**Figure 2a, groups 1-5**). Transfection with S-A<sup>GSK</sup> *Eif2be*, which resulted in a level of total *Eif2be* mRNA (wild-type + mutant) that was approximately twice the endogenous level (**Figure 2a, right**), mimicked the effect of LPS in terms of suppressing CHOP expression (**Figure 2a, group 6**). Transfection with wild-type *Eif2be* also resulted in CHOP suppression (**Figure 2a, group 7**), but the level of suppression was somewhat less than that seen with S-A<sup>GSK</sup> *Eif2be*. Thus, increasing eIF2B $\epsilon$  in ER-stressed MEFs, especially when the  $\epsilon$  subunit cannot be phosphorylated, mimics the effect of LPS on CHOP suppression.

We then conducted a series of experiments in which we first silenced endogenous eIF2B $\epsilon$  using an siRNA that targets mouse but not human (h) *EIF2BE*, followed by transfection of these cells with one of various h*EIF2BE* constructs. The siRNA effectively silenced endogenous eIF2B $\epsilon$ , and the decrease in eIF2B $\epsilon$  was associated with a decrease in LPS-induced CHOP suppression (**Figure 2b, upper left**). This finding is consistent with the model, because there would be very little GEF to be activated by the eIF2B $\epsilon$  dephosphorylation pathway.

We next transfected the silenced cells with a construct encoding human eIF2B $\epsilon$  with S-A point mutations in both the GSK site and an upstream Ser residue, which, when phosphorylated by the kinase DYRK, promotes phosphorylation of the GSK site<sup>8,9</sup> (S-A<sup>GSK/DYRK</sup>). This mutant, which cannot be phosphorylated, should be in a constitutively active state that should promote “resistance” to p-eIF2 $\alpha$  and thereby blunt ER stress-induced CHOP induction (see Figure 2a). Most importantly, if LPS suppresses CHOP by decreasing eIF2B $\epsilon$  phosphorylation, it should have little effect in these cells, because, in the absence of phosphorylation, the mutant cannot be dephosphorylated. The data bear out this prediction: compared with MEFs transfected with WT h*EIF2BE*, those transfected with S-A<sup>GSK/DYRK</sup> h*EIF2BE* showed lower CHOP expression in response to tunicamycin and no significant further decrease of CHOP with LPS pre-treatment (**Figure 2b, upper right**). Finally, using S-D mutants to mimic constitutive phosphorylation, we showed that transfection with S-D<sup>GSK/DYRK</sup> EIF2BE did not restore LPS-induced CHOP suppression in *Eif2be*-silenced MEFs (**Figure 2b, lower left**). Note that the level of total eIF2B $\epsilon$  in cells with silenced endogenous protein plus transfected human protein was similar to the level of endogenous eIF2B $\epsilon$  in non-silenced, non-transfected cells (**Figure 2b, lower right**). These combined data provide further evidence that eIF2B $\epsilon$  dephosphorylation plays an important role in LPS-mediated suppression of CHOP in ER-stressed cells.

In theory, LPS could lead to decreased p-eIF2B $\epsilon$  by decreasing GSK3 activity. However, we found that LPS did not increase the inactive phosphorylated form of GSK3 $\beta$  (**Figure S2a**) or GSK3 $\alpha$ . Moreover, treatment with the PI3-kinase inhibitor LY294002, which activates GSK3 $\beta$ <sup>11</sup>, did not prevent the LPS-mediated suppression of CHOP (data not shown). These data suggested that a phosphatase might be involved, which we tested by incubating cell extracts with [<sup>32</sup>P]eIF2B $\epsilon$  and monitoring the rate of <sup>32</sup>P-dephosphorylation. LPS treatment enhanced dephosphorylation in WT but not *Trif*<sup>-/-</sup> macrophages (**Figure 3a**). Moreover, the enhanced dephosphorylation was suppressed by the phosphatase inhibitor okadaic acid (**Figure 3a**) but not by inhibitors of MAPK phosphatase 1, PP1, and PP2B (data not shown). Because okadaic acid can inhibit PP2A, we tested the effect of siRNA-mediated silencing of the catalytic “C” subunit of PP2A. Compared with scrambled RNA, *Pp2ac* siRNA prevented the LPS-mediated decrease in both p-eIF2B $\epsilon$  and CHOP in ER-stressed macrophages (**Figure 3b**). Note that *Pp2ac* siRNA also prevented the LPS-mediated decrease in ATF4 (**Figure S2b**), which we showed previously is the most proximal translational target of the “p-eIF2 $\alpha$  resistance” pathway<sup>3</sup>. Finally, we found that a constitutively active mutant of PP2A with a Y307F mutation in the catalytic subunit<sup>12</sup> was able to mimic the effect of LPS on suppression of CHOP (**Figure 3c, left**). Conversely, a dominant-negative mutant with an L199P mutation in the catalytic subunit<sup>13</sup> prevented LPS-

mediated CHOP suppression (**Figure 3c, right**). These combined results provide evidence for a pathway in which LPS pre-treatment of ER-stressed cells activates PP2A-mediated dephosphorylation of eIF2B $\epsilon$ , resulting in suppression of CHOP.

PP2A can be activated by an increase in the expression of one or more of its 3 subunits; a decrease in the association of PP2Ac with the inhibitors ANP32 or alpha-4<sup>14,15</sup>; or dephosphorylation of the catalytic subunit at Tyr-307<sup>16</sup>. LPS pretreatment did not affect the expression of any of the PP2A subunits or association of PP2Ac with ANP32 or alpha-4 (data not shown). However, LPS pretreatment led to a subtle but reproducible and statistically significant decrease pTyr-307-PP2Ac in wild-type but not *Trif*<sup>-/-</sup> macrophages (**Figure 3d**). To test this point *in vivo*, we took advantage of the fact that LPS pre-treatment of tunicamycin-treated mice suppresses CHOP expression, but not eIF2 $\alpha$  phosphorylation, in the liver and kidney in a TRIF-dependent manner<sup>3</sup>. We found that LPS pre-treatment led to a decrease in p-eIF2B $\epsilon$  and p-PP2Ac in liver and kidney extracts of tunicamycin-treated mice (**Figure 3e-f**), similar to our observations in cultured macrophages and MEFs.

Src-family kinases (SFKs) can phosphorylate PP2Ac at Tyr-307 and thereby inhibit PP2A phosphatase activity<sup>16-18</sup>, and so a decrease in SFK activity could be a mechanism of PP2A activation. Consistent with this possibility, we found that LPS partially decreased phospho-Tyr-p60<sup>c-src</sup> (p-Src), a measure of Src activation<sup>19</sup>, in wild-type but not *Trif*<sup>-/-</sup> macrophages (**Figure 4a**) and inhibited the kinase activity of immunoprecipitated Src (**Figure 4b**). Poly(I:C), a ligand for the TLR3-TRIF pathway that is a potent suppressor of CHOP in ER-stressed macrophages<sup>3</sup>, also promoted the dephosphorylation of both Src and PP2Ac (**Figure S2c**). To determine causation, we tested the effect of a phosphopeptide (EPQ[pY]EEIPIYL) that activates SFKs by binding to and inhibiting their auto-inhibitory SH2 domains<sup>20,21</sup> and found that it abrogated LPS-induced suppression of both p-PP2Ac and CHOP without increasing p-eIF2 $\alpha$  (**Figure 4c**). The changes in CHOP protein seen with LPS and Src activator treatment were paralleled by changes in *Chop* mRNA (**Figure 4c, bottom right graph**), which is consistent with the fact that the overall pathway involves ATF4-induced *Chop* mRNA<sup>3</sup>. Moreover, the “p-eIF2 $\alpha$  resistance” hypothesis predicts that activation of SFKs would prevent LPS-induced enhancement of global translation in ER-stressed cells<sup>3</sup>. Indeed, by quantifying newly synthesized [<sup>35</sup>S]-labeled proteins, we found that the SFK peptide activator abrogated the LPS-induced increment in new protein translation in tunicamycin-treated macrophages (**Figure 4d**).

To test whether SFK inhibition could mimic the effect of LPS, ER-stressed cells were treated with the SFK inhibitors, PP1 or Su6656, and each were found to suppress p-PP2Ac and CHOP in the absence of LPS (**Figure 4e**). Similar data were obtained using immunofluorescence microscopy assays: LPS treatment led to a decrease in the p-Src signal in wild-type but not *Trif*<sup>-/-</sup> macrophages either in the absence or presence of tunicamycin (**Figures S2d-e**), and both LPS and PP1 decreased the p-PP2Ac signal in tunicamycin-treated cells (**Figure S2f**). As further evidence for the role of SFKs in the pathway, we found that CHOP suppression by the SFK inhibitors was lessened substantially by *Pp2ac* silencing (**Figure S3a**), indicating that this action of the SFK inhibitors requires PP2Ac. Moreover, MEFs transfected with a dominant-negative form of Src (K296R-Y528F) that acts as a pan-SFK inhibitor<sup>22</sup> mimicked the ability of LPS to suppress tunicamycin-induced

CHOP expression (**Figure S3b**). This construct also suppressed hepatic p-PP2Ac, p-eIF2B $\epsilon$ , and CHOP when introduced into the tunicamycin mouse model described above (**Figure S3c**). These combined data provide strong support for the role of SFK inhibition in the TLR-PP2A-eIF2B $\epsilon$ -CHOP pathway.

We speculate that this TRIF-CHOP suppression pathway protects cells from CHOP-induced apoptosis during LPS-induced sepsis. Indeed, when the pathway is disabled by TRIF deficiency in high-dose (hd) LPS-treated mice, where hd-LPS is both the inducer of ER stress and the activator of the TLR-TRIF-CHOP suppression pathway, we observed elevated CHOP, cell death, and organ dysfunction in spleen, liver, and kidney<sup>3</sup>. In hd-LPS-treated macrophages, where CHOP expression and apoptosis were suppressed in WT but not *Trif*<sup>-/-</sup> macrophages (**Figure 5a**), phosphorylation of PP2Ac, eIF2B $\epsilon$ , and p-Src was subtly but reproducibly reduced in a TRIF-dependent manner (**Figure 5b and S4a-c**). Moreover, hd-LPS treatment of wild-type, but not *Trif*<sup>-/-</sup> mice, caused a marked decrease in both p-PP2Ac and p-eIF2B $\epsilon$  in liver (**Figure 5c**) and kidney (data not shown). As tests of causation, we found that *Pp2ac* siRNA and Src activator peptide increased CHOP expression in hd-LPS-treated macrophages, and the Src activator also increased CHOP-dependent apoptosis (**Figure 5d-e**).

We hypothesize that the pathway also maintains uninterrupted synthesis of key proteins needed for a proper LPS-induced inflammatory response by promoting “resistance” to the translational inhibitory effect of p-eIF2 $\alpha$  (see Figure 4d). We first showed that TRIF deficiency blocked the hd-LPS-induced increase in secreted, immunoreactive stimulated TNF $\alpha$  (**Figure S4d**). To distinguish between transcriptional and translational regulation, we conducted a [<sup>35</sup>S]methionine-cysteine labeling experiment and found that hd-LPS increased labeled [<sup>35</sup>S]TNF $\alpha$  in the medium of WT but not *Trif*<sup>-/-</sup> macrophages (**Figure S4e**). This result cannot be explained by decreased processing or secretion of TNF $\alpha$  in *Trif*<sup>-/-</sup> macrophages, because approximately equal amount of immunoprecipitated TNF $\alpha$  protein were loaded in each lane of the gel. Most importantly, when we directly examined newly translated TNF $\alpha$  by conducting a short-term labeling experiment at a time when *Tnfa* mRNA levels were similar among all groups (**inset to Figure 5f**), we found a marked decrease in newly translated pro-TNF $\alpha$ . Together, these data support the idea that the TRIF pathway described herein enables uninterrupted translation of *Tnfa* mRNA.

The data in this report provide evidence for an eIF2B dephosphorylation-GEF activation pathway that initially involves SFK de-activation and then PP2A activation (**Figure S5**). We reason that activation of eIF2B by this pathway boosts GTP exchange on eIF2 enough to enable proper ternary complex cycling despite the presence of p-eIF2 $\alpha$ <sup>8,23</sup>. One possibility is that  $\epsilon$ -dephosphorylated eIF2B can exchange GDP for GTP with higher-than-normal efficiency on the subpopulation of eIF2 complexes whose  $\alpha$ -subunit escapes PERK-mediated phosphorylation, thus compensating for the translation-inhibitory and CHOP-inducing effects of the eIF2 complexes whose  $\alpha$ -subunit is phosphorylated. Another possibility is that dephosphorylated eIF2B could carry out its GEF function on eIF2 complexes that do have  $\alpha$ -subunit phosphorylation, *e.g.*, through a conformation change in dephosphorylated eIF2B that might increase its off-rate from the inhibitory site on p-eIF2 $\alpha$  and this enable GDP-GTP exchange on the  $\gamma$ -subunit of eIF2. Regardless of mechanism,

restoration of protein translation initiation would both suppress ATF4-CHOP and maintain a normal rate of global protein translation. To the extent that the pathway enables LPS-activated macrophages to carry out essential protein translation, it likely works in concert with complementary LPS-induced mechanisms that enhance translation initiation, such as mTOR-induced phosphorylation of 4E-BP1, which activates the initiation factor eIF4E<sup>24</sup>.

The mechanism of SFK deactivation by TLR-TRIF signaling will require further investigation, but our previous findings suggest that IRF5 and IRF7, but not IRF3, should have a role<sup>3</sup>. Interestingly, other studies have reported that LPS can *activate* SFKs, which, based upon the use of chemical inhibitors of SFKs in these reports, may be involved in certain LPS signaling pathways<sup>25-27</sup>. However, these studies are distinguished from the one here by their use of a much shorter LPS incubation time (30 min vs. 14-24 h here). We found that the minimum LPS pre-incubation time that decreased pTyr 416-Src was 8 h, which is consistent with the time of LPS pre-treatment required for CHOP suppression<sup>3</sup>. This lag time may reflect the signaling events downstream of TLR-TRIF needed for LPS or poly(I:C) to induce the change in SFK activity. Moreover, previous studies in this area used an immortalized cell line derived from a leukemia virus-induced tumor (RAW 264.7) or retrovirus-immortalized bone marrow cells instead of primary macrophages. We found that ER-stressed tumor cell-derived cell lines, including RAW 264.7 cells, are not responsive to the CHOP-suppressive effect of pathophysiologic relevant doses of LPS (C. W. Woo and I. Tabas, unpublished data).

Future investigations will test the relevance of this pathway to advanced atherosclerosis, where CHOP-induced macrophage apoptosis promotes plaque necrosis, a key feature of clinically dangerous plaques<sup>28</sup>. In advanced atherosclerotic lesions, macrophage CHOP expression is very high despite the presence of numerous TLR ligands and evidence of macrophage TLR-TRIF activation<sup>28,29</sup>. Therefore, we speculate that the CHOP-suppressive pathway becomes disabled in this setting, perhaps due to interruption of one of the signaling components identified herein. Conversely, tumor cells, which often show evidence of UPR activation without UPR-induced apoptosis, can become resistant to the protein translation-inhibiting effects of p-eIF2 $\alpha$  in the absence of LPS<sup>30</sup>. In one study with human breast cancer cells, this process was associated with an increase in the amount of eIF2B protein<sup>31</sup>, but it is possible that activation of eIF2B $\epsilon$  by dephosphorylation might play a role in “p-eIF2 $\alpha$  resistance” in other types of cancer cells. If so, strategies to disable eIF2B GEF-activating pathways that render cells resistant to p-eIF2 $\alpha$ , such as the one described here, may decrease the resistance of certain types of cancer cells to ER stress-induced cell death<sup>32</sup>. Thus, with further knowledge of the pathway described here, pharmacologic manipulation in one direction or the other may have unique therapeutic potential.

## METHODS

Methods are available in Supplementary Information online.

## Supplementary Material

Refer to Web version on PubMed Central for supplementary material.

## ACKNOWLEDGMENTS

This work was supported by post-doctoral fellowship grants from the Canadian Institutes of Health Research and the Heart & Stroke Foundation of Canada (C.W.W.); NIH-NHLBI grants HL75662 and HL57560 (I.T.); and NIH-NIDDK grants DK13499 and DK15658 (S.R.K.). We thank Dr. David Ron (University of Cambridge) for helpful discussions and for providing the CHOP-GFP reporter plasmid; Dr. Christopher Proud (University of Southampton) for recombinant GST-DYRK2; Dr. Dejian Ren (University of Pennsylvania) for advice regarding the use of mutant Src constructs; Dr. David L. Brautigan (University of Virginia School of Medicine) for the construct encoding Y307F PP2Ac; Dr. Brian A. Hemmings (Friedrich Miescher Institute, Basel, Switzerland) for the construct encoding L199P PP2Ac; and Dr. Brad Berk (University of Rochester) for an adenoviral vector encoding kinase-inactive Src.

## References

1. Todd DJ, Lee AH, Glimcher LH. The endoplasmic reticulum stress response in immunity and autoimmunity. *Nat. Rev. Immunol.* 2008; 8:663–674. [PubMed: 18670423]
2. Ron D, Walter P. Signal integration in the endoplasmic reticulum unfolded protein response. *Nat. Rev. Mol. Cell Biol.* 2007; 8:519–529. [PubMed: 17565364]
3. Woo CW, et al. Adaptive suppression of the ATF4-CHOP branch of the unfolded protein response by toll-like receptor signaling. *Nature Cell Biol.* 2009; 11:1473–1480. PMC2787632. [PubMed: 19855386]
4. Ron D. Translational control in the endoplasmic reticulum stress response. *J. Clin. Invest.* 2002; 110:1383–1388. [PubMed: 12438433]
5. Tabas I, Ron D. Molecular mechanisms integrating pathways of endoplasmic reticulum stress-induced apoptosis. *Nat. Cell Biol.* 2011; 13:184–190. PMC3107571. [PubMed: 21364565]
6. Oyadomari S, Mori M. Roles of CHOP/GADD153 in endoplasmic reticulum stress. *Cell Death. Differ.* 2004; 11:381–389. [PubMed: 14685163]
7. Krishnamoorthy T, Pavitt GD, Zhang F, Dever TE, Hinnebusch AG. Tight binding of the phosphorylated alpha subunit of initiation factor 2 (eIF2alpha) to the regulatory subunits of guanine nucleotide exchange factor eIF2B is required for inhibition of translation initiation. *Mol. Cell Biol.* 2001; 21:5018–5030. [PubMed: 11438658]
8. Welsh GI, Miller CM, Loughlin AJ, Price NT, Proud CG. Regulation of eukaryotic initiation factor eIF2B: glycogen synthase kinase-3 phosphorylates a conserved serine which undergoes dephosphorylation in response to insulin. *FEBS Lett.* 1998; 421:125–130. [PubMed: 9468292]
9. Wang X, Proud CG. A novel mechanism for the control of translation initiation by amino acids, mediated by phosphorylation of eukaryotic initiation factor 2B. *Mol. Cell Biol.* 2008; 28:1429–1442. [PubMed: 18160716]
10. Hardt SE, Tomita H, Katus HA, Sadoshima J. Phosphorylation of eukaryotic translation initiation factor 2Bepsilon by glycogen synthase kinase-3beta regulates beta-adrenergic cardiac myocyte hypertrophy. *Circ. Res.* 2004; 94:926–935. [PubMed: 15001529]
11. Fang X, et al. Phosphorylation and inactivation of glycogen synthase kinase 3 by protein kinase A. *Proc Natl Acad Sci U S A.* 2000; 97:11960–11965. [PubMed: 11035810]
12. Chung H, Nairn AC, Murata K, Brautigan DL. Mutation of Tyr307 and Leu309 in the protein phosphatase 2A catalytic subunit favors association with the alpha 4 subunit which promotes dephosphorylation of elongation factor-2. *Biochemistry.* 1999; 38:10371–10376. [PubMed: 10441131]
13. Evans DR, Myles T, Hofsteenge J, Hemmings BA. Functional expression of human PP2Ac in yeast permits the identification of novel C-terminal and dominant-negative mutant forms. *J. Biol. Chem.* 1999; 274:24038–24046.
14. Santa-Coloma TA. Anp32e (Cpd1) and related protein phosphatase 2 inhibitors. *Cerebellum.* 2003; 2:310–320. [PubMed: 14964690]
15. Nanahoshi M, et al. Alpha4 protein as a common regulator of type 2A-related serine/threonine protein phosphatases. *FEBS Lett.* 1999; 446:108–112. [PubMed: 10100624]
16. Chen J, Martin BL, Brautigan DL. Regulation of protein serine-threonine phosphatase type-2A by tyrosine phosphorylation. *Science.* 1992; 257:1261–1264. [PubMed: 1325671]

17. Hu X, et al. Src kinase up-regulates the ERK cascade through inactivation of protein phosphatase 2A following cerebral ischemia. *BMC. Neurosci.* 2009; 10:74. [PubMed: 19602257]
18. Barisic S, Schmidt C, Walczak H, Kulms D. Tyrosine phosphatase inhibition triggers sustained canonical serine-dependent NFkappaB activation via Src-dependent blockade of PP2A. *Biochem. Pharmacol.* 2010; 80:439–447. [PubMed: 20450893]
19. Brown MT, Cooper JA. Regulation, substrates and functions of src. *Biochim. Biophys. Acta.* 1996; 1287:121–149. [PubMed: 8672527]
20. Liu X, et al. Regulation of c-Src tyrosine kinase activity by the Src SH2 domain. *Oncogene.* 1993; 8:1119–1126. [PubMed: 7683128]
21. Lu B, et al. Peptide neurotransmitters activate a cation channel complex of NALCN and UNC-80. *Nature.* 2009; 457:741–744. [PubMed: 19092807]
22. Encinas M, et al. c-Src is required for glial cell line-derived neurotrophic factor (GDNF) family ligand-mediated neuronal survival via a phosphatidylinositol-3 kinase (PI-3K)-dependent pathway. *J. Neurosci.* 2001; 21:1464–1472. [PubMed: 11222636]
23. Mayhew DL, Hornberger TA, Lincoln HC, Bamman MM. Eukaryotic initiation factor 2B epsilon induces cap-dependent translation and skeletal muscle hypertrophy. *J. Physiol.* 2011; 589:3023–3037. [PubMed: 21486778]
24. Potter MW, Shah SA, Elbirt KK, Callery MP. Endotoxin (LPS) stimulates 4EBP1/PHAS-I phosphorylation in macrophages. *J Surg. Res.* 2001; 97:54–59. [PubMed: 11319880]
25. Lee JY, et al. The regulation of the expression of inducible nitric oxide synthase by Src-family tyrosine kinases mediated through MyD88-independent signaling pathways of Toll-like receptor 4. *Biochem. Pharmacol.* 2005; 70:1231–1240.
26. Kim JY, et al. Src-mediated regulation of inflammatory responses by actin polymerization. *Biochem. Pharmacol.* 2010; 79:431–443. [PubMed: 19769947]
27. Tu S, Wu WJ, Wang J, Cerione RA. Epidermal growth factor-dependent regulation of Cdc42 is mediated by the Src tyrosine kinase. *J Biol Chem.* 2003; 278:49293–49300. [PubMed: 14506284]
28. Moore KJ, Tabas I. Macrophages in the pathogenesis of atherosclerosis. *Cell.* 2011; 145:341–355. PMC3111065. [PubMed: 21529710]
29. Curtiss LK, Tobias PS. Emerging role of toll-like receptors in atherosclerosis. *J. Lipid Res.* 2008
30. Lee AS, Hendershot LM. ER stress and cancer. *Cancer Biol. Ther.* 2006; 5:721–722. [PubMed: 16880733]
31. Check J, et al. Src kinase participates in LPS-induced activation of NADPH oxidase. *Mol. Immunol.* 2010; 47:756–762. [PubMed: 19942291]
32. Healy SJ, Gorman AM, Mousavi-Shafaei P, Gupta S, Samali A. Targeting the endoplasmic reticulum-stress response as an anticancer strategy. *Eur. J Pharmacol.* 2009; 625:234–246. [PubMed: 19835867]



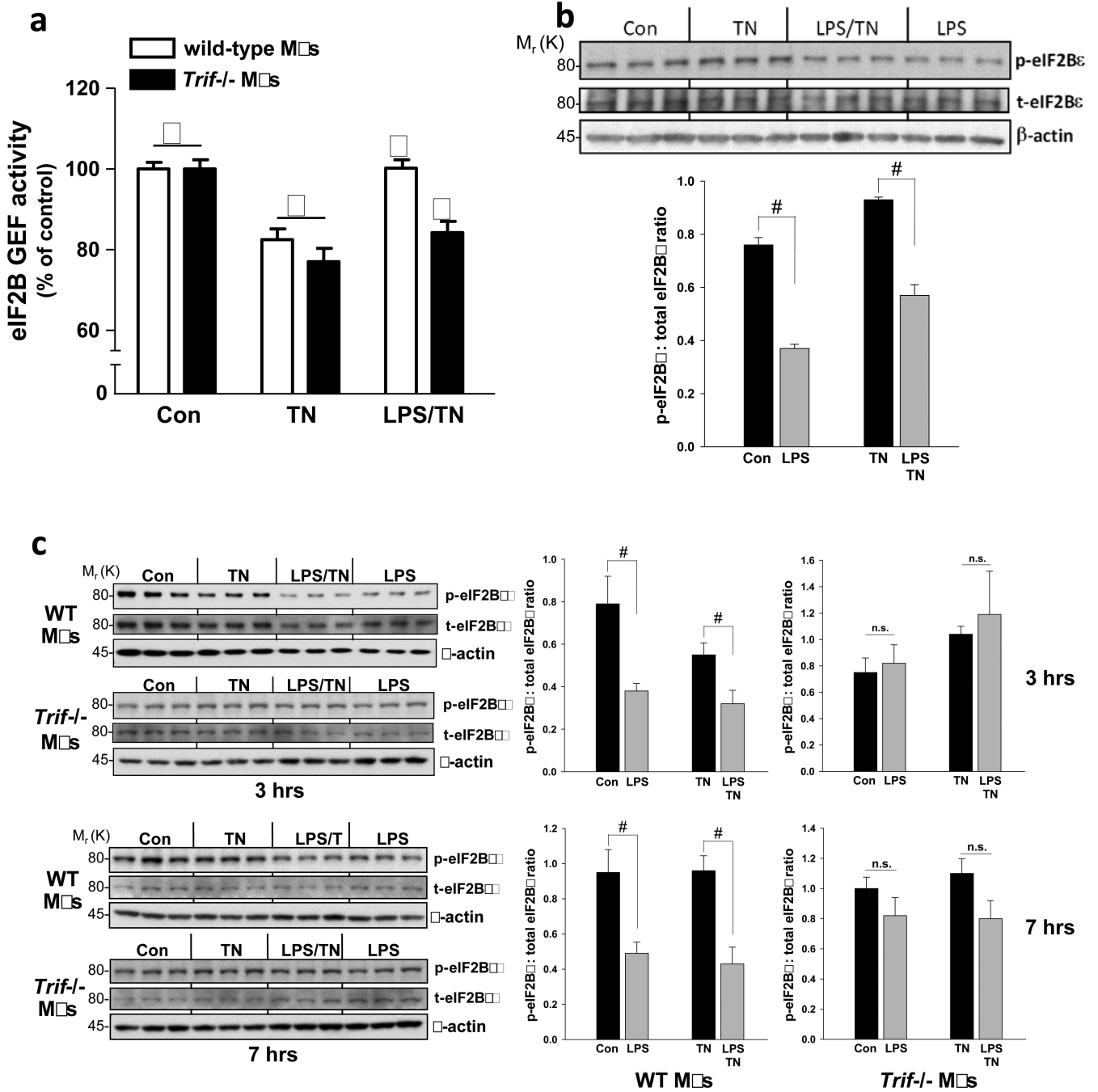


**Figure 1.**

LPS increases guanine nucleotide exchange activity of eIF2B. (a) Macrophages from wild-type or *Trif*<sup>-/-</sup> mice were untreated or pretreated with LPS (1 ng ml<sup>-1</sup>) for 24 h followed by a 3-h treatment with tunicamycin (TN, 1 μg ml<sup>-1</sup>). eIF2B GEF activity was then assayed. Data are expressed as mean ± s.e.m. with n = 6; bars with different symbols are statistically different from each other, P < 0.02. (b) Cells were treated similarly to those in (a), except an LPS-only group was included, and then extracts were analyzed by immunoblot analysis for phospho (p)- and total (t) eIF2Bε and β-actin as loading control. Densitometric

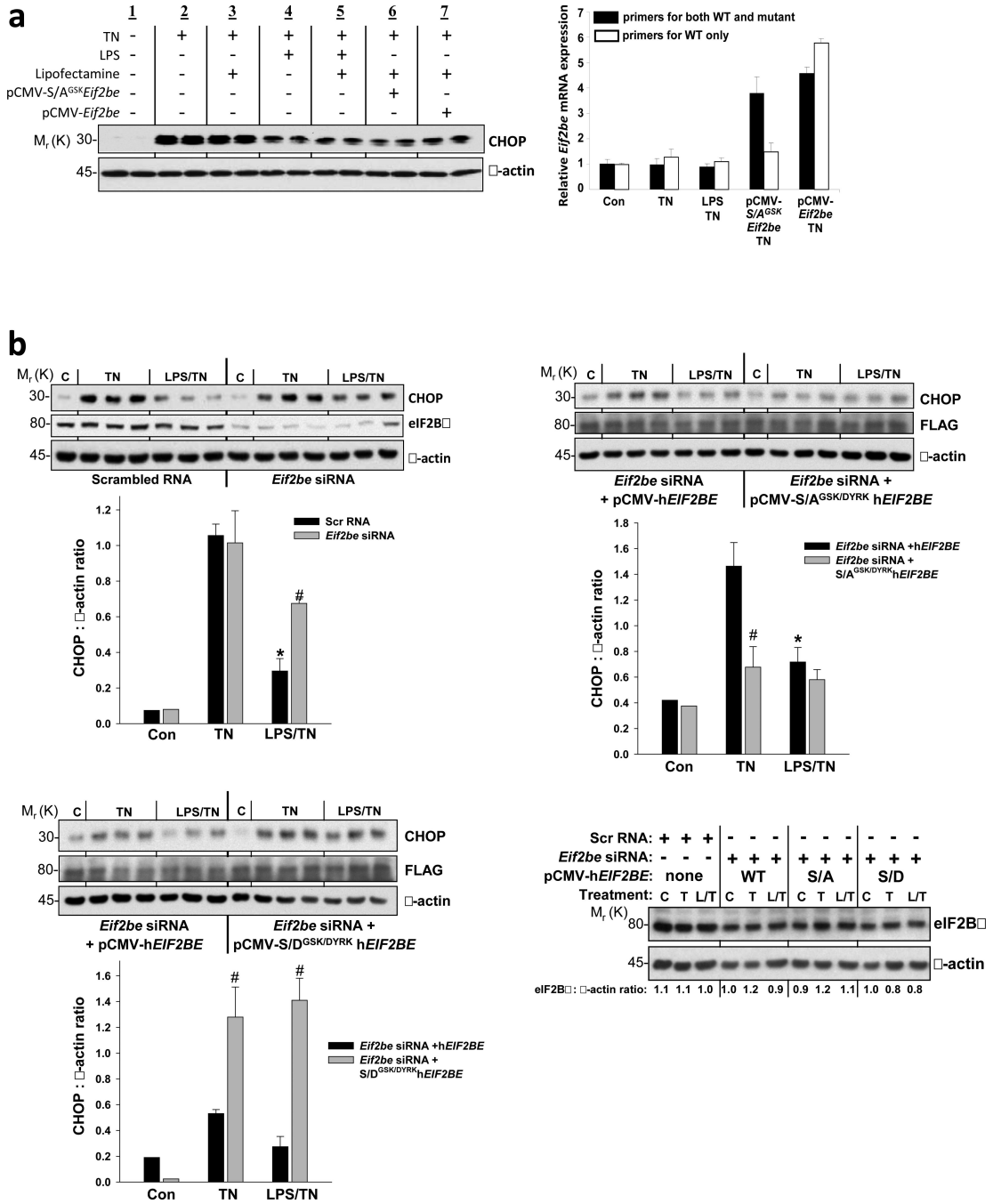
quantification of the immunoblot data are shown in the graph as mean  $\pm$  s.e.m. with  $n=3$ . #,  $P < 0.05$ . (c) As in (b), except macrophages from wild-type and *Trif*<sup>-/-</sup> mice were compared, and data for 7 h of tunicamycin treatment are also shown. #,  $P < 0.05$ ; n.s., non-significant.

Author Manuscript

Author Manuscript

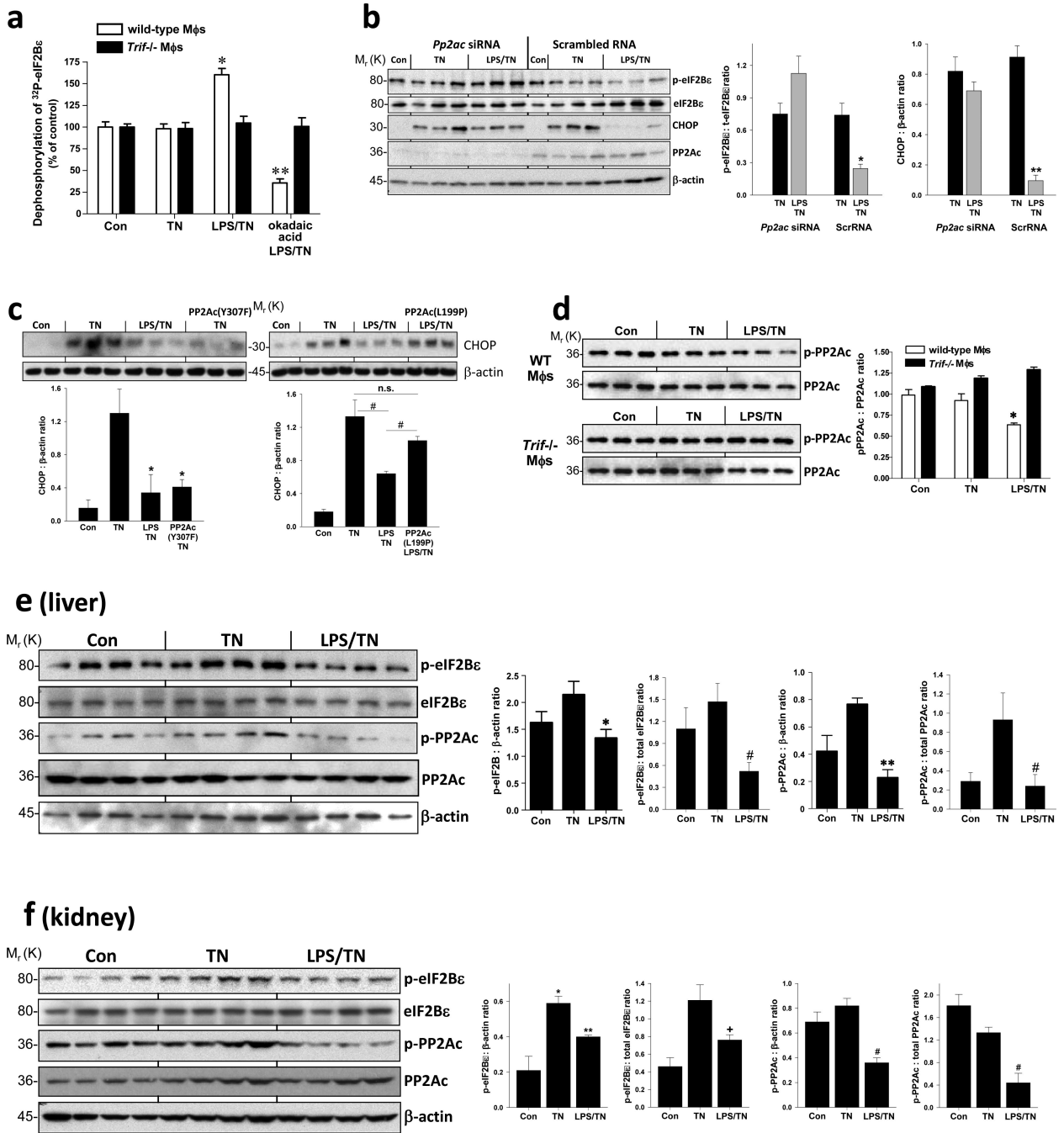
Author Manuscript

Author Manuscript



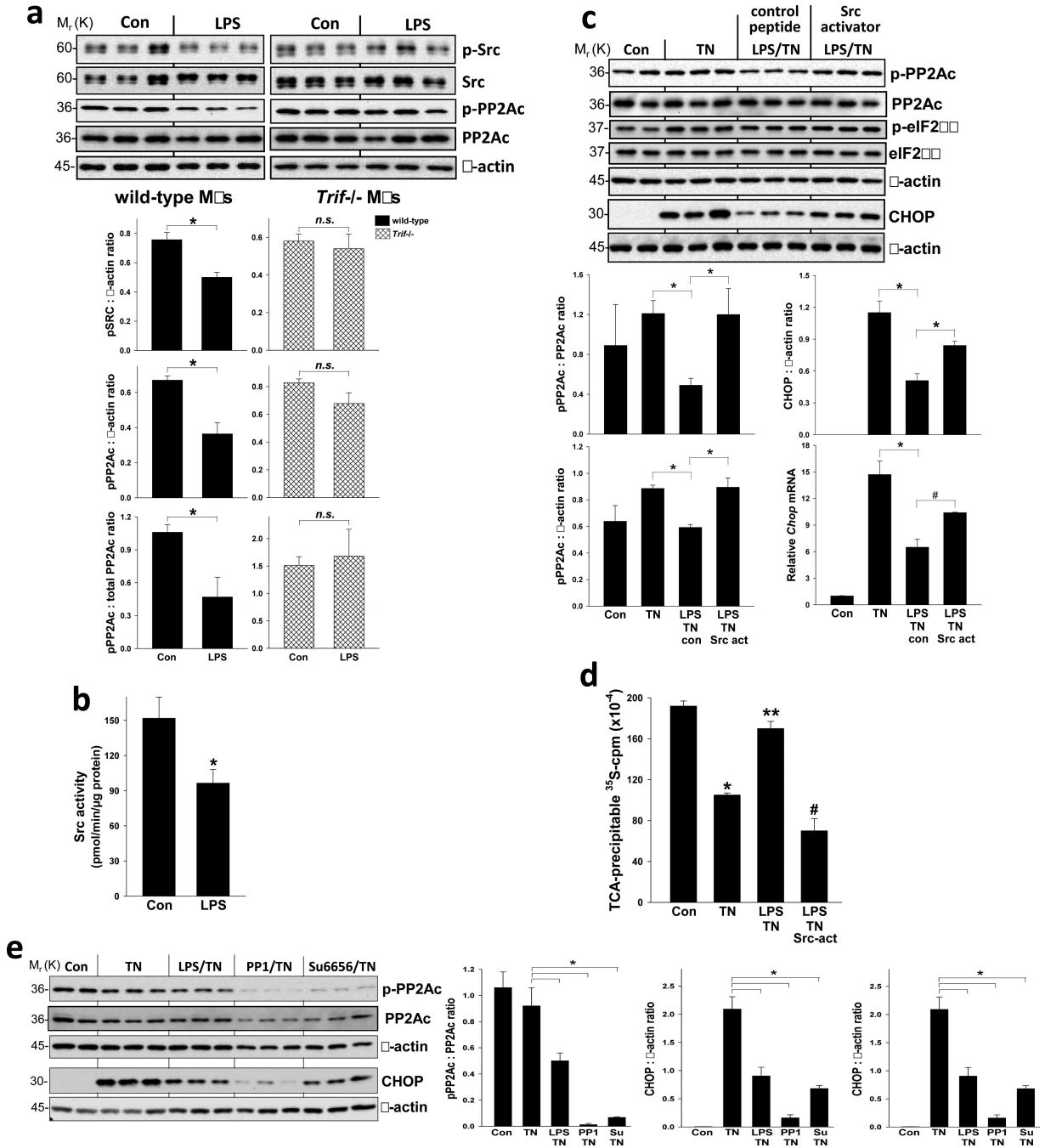
**Figure 2.** Evidence that dephosphorylation of eIF2Bε is involved in LPS-mediated CHOP suppression in ER-stressed MEFs. (a) MEFs were treated under the indicated conditions, and then cell extracts were analyzed by immunoblot for CHOP and β-actin. The conditions were the same as those in Fig. S1a (8 h ± LPS then 2 h tunicamycin) except that the cells in lanes 3 and 5 first underwent mock transfection (Lipofectamine) while those in 6-7 were transfected with plasmids encoding rat *Eif2be* with a Ser-Ala mutation in the GSK3β phospho-site (S-A<sup>GSK</sup>) or wild-type *Eif2be*. The graph to the right shows the levels of total (black bars) and wild-

type (WT)-only (white bars) *Eif2be* mRNA from MEFs incubated under the indicated conditions. The mRNA data are from duplicate samples per group, and the duplicate values varied by <10% for all 10 groups. **(b)** In **(upper left)**, MEFs were transfected with scrambled RNA or murine *Eif2be* siRNA, and in **(upper right and lower left)**, *Eif2be*-silenced MEFs were then transfected with a plasmid encoding WT human eIF2B $\epsilon$  or human eIF2B $\epsilon$  with S-A (upper left) or S-D (lower right) mutations in the GSK and DYRK sites (S-A<sup>GSK/DYRK</sup> and S-D<sup>GSK/DYRK</sup>, respectively). Twelve hours after transfection with the wild-type or mutant hEIF2BE plasmids, the cells were pretreated for 8 h in the absence or presence of LPS (500 ng ml<sup>-1</sup>) and then incubated for 2 h in control medium (C) or in medium containing tunicamycin (TN, 0.5  $\mu$ g ml<sup>-1</sup>). Extracts were subjected to immunoblot analysis for CHOP, eIF2B $\epsilon$  or FLAG, and  $\beta$ -actin. Densitometric quantification of the immunoblot data are shown in the graphs as mean  $\pm$  s.e.m. with n=3. \*P < 0.05 vs. TN; #P < 0.05 vs. scrambled RNA (upper left) or vs. wild-type hEIF2BE groups (upper right and lower panel). **(Lower right)** Total eIF2B $\epsilon$  (with  $\beta$ -actin loading control) in samples from the experiments in upper panel and lower left; densitometric quantification of each lane appears below that lane. C, control; L, LPS; T, tunicamycin.

**Figure 3.**

LPS promotes dephosphorylation of eIF2Bε through a mechanism involving PP2A, with evidence *in vivo*. (a) Macrophages from wild-type or *Trif*<sup>-/-</sup> mice were untreated or pretreated ± LPS (1 ng ml<sup>-1</sup>) for 24 h followed by treatment with tunicamycin (TN, 1 μg ml<sup>-1</sup>) for 90 min. In an additional LPS-TN group, the phosphatase inhibitor okadaic acid (1 nM) was added at the same time as LPS. Cells extracts were then added to a solution of purified <sup>32</sup>P-labeled eIF2Bε, and the rate of dephosphorylation was determined as described in Methods. Data are expressed as mean ± s.e.m. with n = 6; \*P < 0.05 compared with Con

and the corresponding *Trif*<sup>-/-</sup> group. \*\*P < 0.05, compared with TN and the corresponding *Trif*<sup>-/-</sup> group. (b) Macrophages were transfected with scrambled RNA or *Pp2ac* siRNA, and 48 h later the cells were treated similarly to the first 3 wild-type groups in (a). Cell extracts were analyzed by immunoblot for p- and total eIF2B $\epsilon$ , CHOP, PP2Ac, and  $\beta$ -actin. The data were then quantified by densitometry. \*P < 0.05 and \*\*P < 0.02 vs. TN in the scrambled RNA groups. (c) MEFs were either mock-transfected or transfected with a plasmid encoding PP2Ac with a Tyr307-Phe mutation or a Leu199-Pro mutation. 12 h post-transfection, cells were then treated  $\pm$  LPS (500 ng ml<sup>-1</sup>) for 8 h followed by a 2-h treatment with tunicamycin (TN; 0.5  $\mu$ g ml<sup>-1</sup>). Cell extracts were subjected to immunoblot analysis for CHOP and  $\beta$ -actin. Densitometric quantification of the immunoblot data are shown in the graph. \*P < 0.001 vs. TN group; #P < 0.03 vs. LPS-TN group; n.s., not significant. (d) Macrophages from wild-type or *Trif*<sup>-/-</sup> mice were untreated or pretreated  $\pm$  LPS (1 ng ml<sup>-1</sup>) for 24 h followed by treatment with tunicamycin (TN, 1  $\mu$ g ml<sup>-1</sup>) for 3 h. Extracts were analyzed by immunoblot for phospho (p)- and total PP2Ac and then quantified by densitometry; \*P < 0.05 vs. control and TN groups for wild-type macrophages and vs. all groups for *Trif*<sup>-/-</sup> macrophages. (e) Mice were injected intravenously with LPS (80  $\mu$ g kg<sup>-1</sup>) or vehicle control once a day for 2 consecutive days and then injected with tunicamycin (TN, 1 mg kg<sup>-1</sup>) intraperitoneally. Twelve hours later, the mice were sacrificed, and liver extracts were assayed by immunoblot for p- and total PP2Ac, p- and total eIF2B $\epsilon$ , and  $\beta$ -actin and then quantified by densitometry. \*P = 0.04; \*\*P = 0.0004; #P = 0.015. (f) As in (e), except the mice were sacrificed 24 h after the tunicamycin injection, and kidney extracts were assayed. \*P = 0.02 compared with Con; \*\*P = 0.04 compared with TN. +P < 0.05 compared with TN; #P < 0.01 compared with TN. All densitometry data are expressed as mean  $\pm$  s.e.m. with n = 3, except n = 4 for (e) and (f).

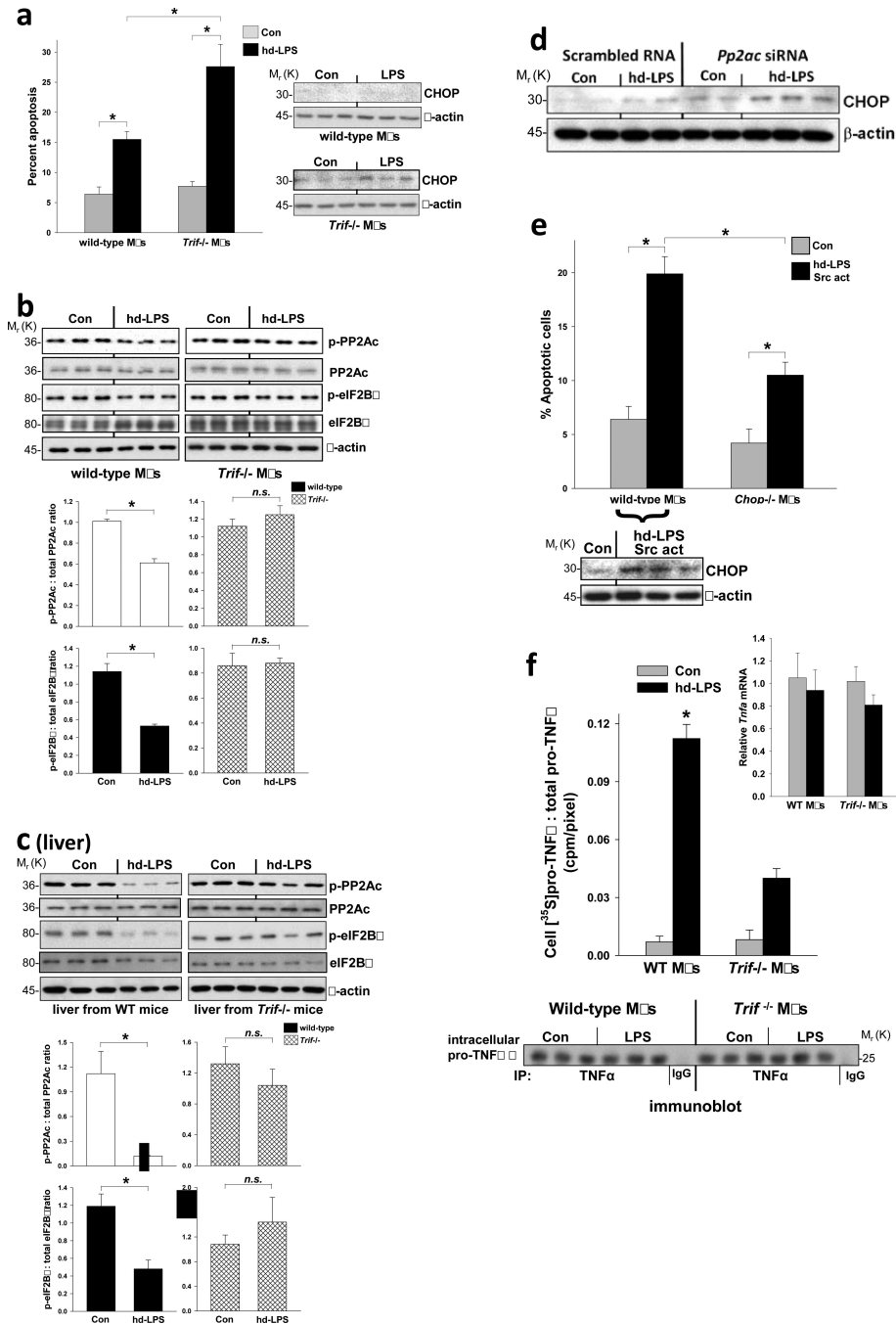


**Figure 4.**

Evidence that TLR-TRIF-mediated PP2Ac de-phosphorylation, CHOP suppression, and restoration of global protein translation involve a pathway involving SFK deactivation. (a) Macrophages from wild-type or *Trif*<sup>-/-</sup> mice were untreated or treated with LPS (1 ng ml<sup>-1</sup>) for 24 h. Extracts were analyzed by immunoblot for phospho-Tyr 416 (p)- and total Src, p- and total PP2Ac, and β-actin and then quantified by densitometry. n = 3; \*P < 0.03. (b) Src was immunoprecipitated from cell extracts of control or LPS-treated macrophages and its kinase activity was then assayed. n = 4; \*P < 0.05. (c) Macrophages were untreated or

pretreated  $\pm$  LPS ( $1 \text{ ng ml}^{-1}$ ) for 24 h followed by treatment with tunicamycin (TN,  $1 \text{ }\mu\text{g ml}^{-1}$ ) for 3 h for PP2Ac, 7 h for CHOP protein, or 5 h for *Chop* mRNA. The LPS-TN or TN groups were pre-treated for 4 h prior to the above incubations with or without control peptide or Src activator peptide under conditions that facilitated their uptake by the cells (see Methods). Extracts were analyzed by immunoblot for p- and total PP2Ac, p- and total eIF2 $\alpha$ , CHOP and  $\beta$ -actin and then quantified by densitometry.  $n = 3$ ; \* $P < 0.05$ . *Chop* mRNA was assayed by QTPCR.  $n = 3$ ; \* $P = 0.015$ ; # $P = 0.04$ . (d) Macrophages were treated under control, TN, LPS-TN, or LPS-TN-Src activator conditions as above. The cells were then pulse-labeled with [ $^{35}\text{S}$ ]methionine-cysteine for 20 min, followed by precipitation with ice-cold TCA and then quantification of  $^{35}\text{S}$ -cpm in the TCA precipitate.  $n = 4$ ; \* $P < 0.05$  compared with Con; \*\* $P < 0.05$  compared with TN; # $P < 0.05$  compared with LPS-TN. (e) Macrophages were untreated or pretreated  $\pm$  LPS ( $1 \text{ ng ml}^{-1}$ ) for 24 h followed by treatment with tunicamycin (TN,  $1 \text{ }\mu\text{g ml}^{-1}$ ) for 3 h (for PP2Ac) or 7 h (for CHOP). Some of the tunicamycin-treated cells were co-treated with the SFK inhibitors PP1 ( $10 \text{ }\mu\text{M}$ ) or Su 66686 ( $20 \text{ }\mu\text{M}$ ). Extracts were analyzed by immunoblot for p- and total PP2Ac, CHOP and b-actin and then quantified by densitometry.  $n = 3$ ; \* $P < 0.05$ . All data are expressed as mean  $\pm$  s.e.m. with  $n$  as indicated above.



**Figure 5.**

Evidence for and functional significance of the TRIF-Src-PP2Ac-eIF2B pathway in a high-dose LPS model. (a) Macrophages from wild-type and *Trif*<sup>-/-</sup> mice were treated for 24 or 28 h in the absence (Con) or presence of high-dose LPS (hd-LPS; 1  $\mu$ g ml<sup>-1</sup>). The cells were then assayed for apoptosis (28 h) or CHOP and  $\beta$ -actin expression (24 h). \* $P < 0.05$ . (b) Additional extracts from the 24-h cells in (a) were analyzed by immunoblot for p- and total PP2Ac, p- and total eIF2B, and  $\beta$ -actin and quantified by densitometry. \* $P < 0.02$ ; n.s., not significant. Similar densitometry data were obtained using  $\beta$ -actin as the loading control (not

displayed). (c) Wild-type or *Trif*<sup>-/-</sup> mice were injected intraperitoneally with PBS control or 5 mg kg<sup>-1</sup> LPS (hd-LPS). Three hours later, liver extracts were assayed for p- and total PP2Ac, p- and total eIF2Bε, and β-actin by immunoblot and quantified by densitometry. \*P < 0.02; *n.s.*, not significant. (d) Macrophages were transfected with scrambled RNA or *Pp2ac* siRNA, and 48 h later the cells were treated with hd-LPS. Extracts were subjected to immunoblot analysis for CHOP and β-actin. (e) Macrophages from wild-type and *Trif*<sup>-/-</sup> mice were treated under control conditions or with hd-LPS at time = 0 and then the Src activator peptide used in Fig. 4c was added at time = 10 h. At time = 24 h, the cells were assayed for apoptosis (n = 3 per group), and extracts from parallel incubations were analyzed by immunoblot for CHOP and β-actin. \*P < 0.01. (f) Macrophages from wild-type and *Trif*<sup>-/-</sup> mice were first treated for a total of 16 h in the absence (Con) or presence of hd-LPS, where the last hour included [<sup>35</sup>S]methionine-cysteine in the medium. Cell extracts were immunoprecipitated using anti-TNFα or IgG control, followed by approximate equal loading of immunoprecipitated TNFα and then anti-TNFα immunoblot. The pro-TNFα band (25 kDa) for each sample on the immunoblot was quantified by densitometry (each band was assigned a pixel value), and then the bands were cut out and counted for [<sup>35</sup>S]cpm. The data were quantified as cpm/pixel. \*P = 0.01 vs. all other groups. *Inset*, *Tnfa* mRNA level at the 16-h timepoint. All data are expressed as mean ± s.e.m. with n = 3.